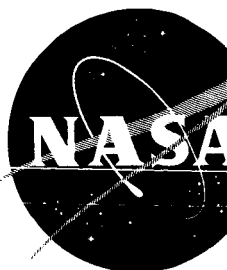


NASA TM X-328

62 7.2152
NASA:EM X-328 591



GPO PRICE \$ _____

OTS PRICE(S) \$ _____

Hard copy (HC) 2.00

Microfiche (MF) 50

298-X

TECHNICAL MEMORANDUM

X-328

EFFECTS OF WING HEIGHT ON THE
STABILITY AND CONTROL CHARACTERISTICS AT A MACH
NUMBER OF 2.01 OF A CANARD AIRPLANE CONFIGURATION
WITH A 70° DELTA WING

By Cornelius Driver

Langley Research Center
Langley Field, Va.

(THRU)

(CODE)

(CATEGORY)

DECLASSIFIED - EFFECTIVE 1-15-64
Authority: Memo Geo. Drobka NASA HQ.
Code ATSS-A Dtd. 3-12-64 Subj: Change
in Security Classification Markings

[REDACTED]

NATIONAL AERONAUTICS AND SPACE ADMINISTRATION.
WASHINGTON

September 1960

N65-12800

(ACCESSION NUMBER)

31

(PAGES)

TMX-328
(NASA OR TMX OR AD NUMBER)

DECLASSIFIED

NATIONAL AERONAUTICS AND SPACE ADMINISTRATION

TECHNICAL MEMORANDUM X-328

EFFECTS OF WING HEIGHT ON THE
STABILITY AND CONTROL CHARACTERISTICS AT A MACH
NUMBER OF 2.01 OF A CANARD AIRPLANE CONFIGURATION
WITH A 70° DELTA WING*

By Cornelius Driver

SUMMARY

An investigation has been made in the Langley 4- by 4-foot supersonic pressure tunnel at a Mach number of 2.01 to determine the effects of wing height on the stability and control characteristics of a canard airplane configuration having wing and canard surfaces of 70° delta planform. The configurations were tested with a vertical tail mounted on the body plane of symmetry and with twin tails mounted on the wing at about the 50-percent-semispan location.

The low-wing configuration with the body-mounted vertical tail had the highest trim values of lift-curve slope, control effectiveness, and lift-drag ratio of the configurations tested.

The positioning of the vertical tails outboard on the wing caused a reversal in the wing-height effects on the directional-stability level, and the high-wing configuration maintained the highest level of directional stability. The presence of the canard surface on the configuration which had the twin vertical tails mounted on the wing had a significantly smaller decrease in directional stability with angle of attack than did the configuration which had the vertical tail on the body.

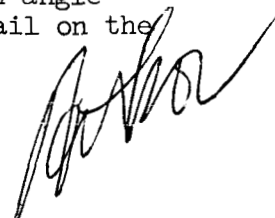
INTRODUCTION

A research program has been under way at the Langley 4-by 4-foot supersonic pressure tunnel to determine the aerodynamic characteristics

*Title, Unclassified.

DECLASSIFIED - EFFECTIVE 1-15-64
Authority: Memo Geo. Drobka NASA HQ.
Code ATSS-A Dtd. 3-12-64 Subj: Change
in Security Classification Marking

12800



of several canard airplane configurations. Various phases of the program are presented in references 1 to 6. As a continuation of the program, an investigation was made to determine the effects of wing vertical location on the aerodynamic characteristics of a configuration with a wing and a canard surface of 70° delta planform. Portions of the present results have previously been reported in reference 7.

The purpose of the present investigation was to determine the extent that the aerodynamic characteristics in pitch and sideslip might be affected by changing the location of the wing-chord plane with respect to the canard wake and the vertical tail. Three vertical locations of the wing were investigated with the vertical tail located on the body plane of symmetry or with twin tails located on the wings.

COEFFICIENTS AND SYMBOLS

The results are referred to the body-axis system except the lift and drag coefficients which are referred to the stability-axis system. The moment reference point is on the body center line 25 inches rearward of the nose of the model.

The coefficients and symbols are defined as follows:

C_L	lift coefficient, $\frac{\text{Lift}}{qS}$
C_D	drag coefficient, $\frac{\text{Drag}}{qS}$
C_m	pitching-moment coefficient, $\frac{\text{Pitching moment}}{qS\bar{c}}$
C_l	rolling-moment coefficient, $\frac{\text{Rolling moment}}{qSb}$
C_n	yawing-moment coefficient, $\frac{\text{Yawing moment}}{qSb}$
C_Y	side-force coefficient, $\frac{\text{Side force}}{qS}$
q	free-stream dynamic pressure, lb/sq ft
S	wing area including body intercept, sq ft

DECLASSIFIED

3

S_c canard area, exposed panel, sq ft
 \bar{c} wing mean geometric chord, in.
 b wing span, in.
 M free-stream Mach number
 α angle of attack, deg
 β angle of sideslip, deg
 δ_c angle of canard deflection (trailing edge down, positive), deg
 L/D lift-drag ratio
 $C_{n\beta}$ directional-stability parameter, $\frac{\partial C_n}{\partial \beta}$
 $C_{l\beta}$ effective-dihedral parameter, $\frac{\partial C_l}{\partial \beta}$
 $C_{Y\beta}$ side-force parameter, $\frac{\partial C_Y}{\partial \beta}$
 $\frac{\partial C_m}{\partial C_L}$ longitudinal-stability parameter

Subscripts:

max maximum

min minimum

Configuration components:

B body

W wing

C canard surface

V vertical tail

03713091030

4

MODELS AND APPARATUS

Details of the model are shown in figure 1, and the geometric characteristics are presented in table I. Coordinates for the body are presented in table II.

The body of the model was composed of a parabolic nose followed by the frustum of a cone which was faired into a cylinder. The fineness ratio of the body was 11.1.

The canard surfaces were 70° delta planforms with hexagonal airfoil sections. The canard surface was motor-driven and the deflections were set by remote control.

The wing also had a 70° delta planform with hexagonal $2\frac{1}{2}$ -percent-thick airfoil sections and was mounted in either a high, mid, or low position. The model was equipped with a swept vertical tail mounted on the body plane of symmetry or with twin swept vertical tails mounted outboard on the wing. Thus, the wing-mounted tails had twice the total area of the body-mounted configuration. For the mid and high wing locations, the wing-mounted vertical tails were located at the $0.538b/2$ position; whereas for the low wing location, the tails were located at the $0.449b/2$ position.

The model was mounted in the tunnel on a remotely controlled rotary sting, and force measurements were made through the use of a six-component internal strain-gage balance.

TESTS, CORRECTIONS, AND ACCURACY

The tests were conducted at a Mach number of 2.01, a stagnation temperature of 100° F, a stagnation pressure of 1,440 lb/sq ft, and a Reynolds number based on the wing mean aerodynamic chord of 3.16×10^6 .

The stagnation dewpoint was maintained sufficiently low (-25° F or less) so that no condensation effects were encountered in the test section.

Tests were made for an angle-of-attack range from 0° to about 20° at $\beta = 0^\circ$ and $\beta = 4^\circ$.

The angles of attack and sideslip were corrected for the deflection of the balance and sting under load. The base pressure was measured, and the drag force was adjusted to a base pressure equal to free-stream static pressure.

The estimated accuracy of the individual measured quantities is as follows:

C_L	± 0.003
C_D	± 0.001
C_m	± 0.0004
C_{l_i}	± 0.0004
C_n	± 0.0001
C_y	± 0.0015
α , deg	± 0.2
β , deg	± 0.2
δ_c , deg	± 0.1
M	± 0.01

DISCUSSION

Longitudinal Characteristics

The basic data for the longitudinal aerodynamic characteristics are presented in figures 2 and 3 and are summarized in figures 4 and 5.

The low-wing configuration had the most desirable longitudinal characteristics of any of the wing positions tested. In fact, for a constant center-of-gravity position (fig. 4), the wing in the low position provided a substantial increase in the trim lift-curve slope over that of the wing in the high position with a corresponding increase in trim $C_{L\delta_c}$ and trim $(L/D)_{\max}$. The increment in trim lift and trim L/D between the mid- and low-wing configurations is smaller than the increment between the mid- and high-wing configurations. The low-wing configuration maintained the highest values of trim L/D throughout the static-margin range (fig. 5). These results are probably due to the interference effect of the wake from the canard surface which provided a significant loss of wing lift near the wing leading edge. (See ref. 5.) For configurations with delta wings where the wing apex extends significantly forward of the center of moments, the loss of lift results in a pitching-moment increment opposite to that provided by the canard surfaces with a corresponding loss in pitch effectiveness and trim L/D .

Since moving the wing leading edge rearward allows the wake from the canard surface to pass above the wing-chord plane at lower angles of attack, a similar effect may also be achieved by moving the wing down. Thus, as the angle of attack of the low-wing configuration increased (fig. 2(c)), the canard-surface wake passed above the wing

and the interference effects were reduced. An indication of the interference effects on the wing is shown by the increasing nonlinearity of the pitching-moment curves with increasing wing height. The high wing, however, remained in the wake from the canard surface through the angle-of-attack range corresponding to $(L/D)_{\max}$, and thus a more adverse effect on the trim values of $C_{L\alpha}$, $C_{L\delta_c}$, and L/D was indicated (fig. 4(a)).

The results for the twin-tail configuration (fig. 4(b)) were similar to the results for the body-mounted-tail configuration. The increased drag caused by the addition of the second vertical tail did result in a lower lift-drag ratio, however.

Lateral Characteristics

The lateral aerodynamic characteristics for the configurations with various wing heights are summarized in figure 6.

Single vertical tail.- The results for the configuration with the single vertical tail on and the canard surface off indicate a significantly higher level of directional stability $C_{n\beta}$ throughout the angle-of-attack range for the low-wing configuration than for the mid- or high-wing configuration because of a substantially greater contribution from the vertical tail. The vertical-tail contribution decreased with increasing angle of attack for all three wing positions. As a result of this decrease and the initial low level of $C_{n\beta}$ for the high-wing configuration, the angle of attack at which $C_{n\beta}$ became zero was lower for the high-wing configuration than for the low- or mid-wing configurations. In general, these results for differences in wing height were similar to those previously reported for conventional swept-wing configurations in references 8 and 9 and for a trapezoidal-wing canard configuration in reference 7. These effects are results of the induced sidewash from the wing-body juncture that, for a high wing location, provided a destabilizing flow above the wing wake and a stabilizing flow below the wing wake and had an opposite effect for the low-wing configuration (refs. 8 and 9).

For the low wing location with the vertical tail on, the presence of the canard surface was destabilizing throughout the angle-of-attack range. For the mid-wing configuration the presence of the canard surface was slightly destabilizing below the angle of attack where $C_{n\beta}$ became zero but was stabilizing above this angle of attack. The presence of the canard for the high-wing configuration resulted in a significant increase in the level of $C_{n\beta}$ because of a decrease in the tail-off instability with increasing angle of attack. With the canard on the

low-wing configuration maintained the highest directional stability level up to about 7° angle of attack. All three wing locations, however, became directionally unstable at about 12° angle of attack.

With the vertical tail off, the effective dihedral parameter C_{l_β} became more negative (at $\alpha = 0^\circ$) with increasing wing height. These results are similar to those reported in references 7 to 9. For all three wing locations, the vertical tail provides an additional increase in effective dihedral. For the low wing location the canard surface provides a further negative increment in C_{l_β} throughout the angle-of-attack range. The complete high-wing configuration had such large values of effective dihedral that provision for effective roll control might present some difficulty.

The side-force parameter C_{Y_β} for the low-wing configuration (tail on) decreased with increasing angle of attack until near 17° where the presence of the vertical tail resulted in little or no increment in side force. The high-wing configuration, which initially had the same side-force level as the other configurations, had an increasing level of side force with angle of attack even though the vertical-tail contribution decreased in a manner similar to that of the low-wing case. The side-force results were in general agreement with the directional-stability and effective-dihedral results.

Twin vertical tails.- The positioning of the vertical tails outboard on the wing to take advantage of the sidewash and canard-surface interference effects resulted in a reversal of the wing-height effects on C_{n_β} shown for the body-mounted vertical tail. For the twin-tail configurations, the high wing location (fig. 6) had the highest level of C_{n_β} at an angle of attack of zero while the low wing location had a significantly lower initial level. All three wing locations (canard surface off) showed a decrease in C_{n_β} with increasing angle of attack and reached neutral stability at about 16° . When the canard surface was added, however, the decrease with angle of attack was alleviated and all three wing locations with the twin tails had a higher C_{n_β} level at an angle of attack of 17° than did the single-vertical-tail configurations near 0° . (Note in fig. 1 that the wing-mounted vertical tails on the low-wing configuration were mounted farther inboard than for the mid- or high-wing configurations.)

The effective dihedral results for the mid-wing configuration with the wing-mounted vertical tails are similar to the results for the body-mounted location. For the low-wing configuration with the wing-mounted

03:41:29.10:30

vertical tails, however, a portion of the vertical-tail area was below the body center line and thus little increase in the negative effective dihedral was indicated. Conversely, for the high-wing configuration the negative level of C_{l_β} was greater for the wing-mounted-tail configuration than for the body-mounted-tail configuration and would present even greater roll-control problems. For all three wing locations the addition of the vertical tails provided a significant increment in side force even at 17° angle of attack.

CONCLUSIONS

An investigation has been made in the Langley 4- by 4-foot supersonic pressure tunnel at a Mach number of 2.01 to determine the effects of wing height on the stability and control characteristics of an airplane configuration having wing and canard surfaces of 70° delta planform. The configurations were tested with vertical tails mounted on the body plane of symmetry and with twin tails mounted at about the 50-percent-semispan location on the wing. The investigation resulted in the following conclusions:

1. The low-wing configuration with the body-mounted vertical tail had the highest trim values of lift-curve slope, control effectiveness, and lift-drag ratio of all the configurations tested.
2. For the configurations with the vertical tail mounted on the body the configuration with the low wing maintained the highest level of directional stability up to about 7° angle of attack.
3. Placing the vertical tails outboard on the wing caused a reversal in the effects of wing height on the directional stability, and the configuration with the high wing maintained the highest level of directional stability.
4. The presence of the canard surface on the configuration which had the vertical tails mounted on the wing resulted in a significantly smaller decrease in directional stability with angle of attack than with the configuration which had the vertical tail on the body.
5. The high-wing configurations had such large values of effective dihedral that provision for effective roll control might present some difficulty.

Langley Research Center,
National Aeronautics and Space Administration,
Langley Field, Va., June 13, 1960.

DECLASSIFIED

9

REFERENCES

1. Driver, Cornelius: Longitudinal and Lateral Stability and Control Characteristics of Two Canard Airplane Configurations at Mach Numbers of 1.41 and 2.01. NACA RM L56L19, 1957.
2. Spearman, M. Leroy, and Driver, Cornelius: Effect of Canard Surface Size on Stability and Control Characteristics of Two Canard Airplane Configurations at Mach Numbers of 1.41 and 2.01. NACA RM L57L17a, 1958.
3. Spearman, M. Leroy, and Driver, Cornelius: Longitudinal and Lateral Stability and Control Characteristics at Mach Number 2.01 of a 60° Delta-Wing Airplane Configuration Equipped With a Canard Control and With Wing Trailing-Edge Flap Controls. NACA RM L58A20, 1958.
4. Spearman, M. Leroy, and Driver, Cornelius: Effects of Forebody Length on the Stability and Control Characteristics at a Mach Number of 2.01 of a Canard Airplane Configuration With a Trapezoidal Aspect-Ratio-3 Wing. NASA MEMO 10-14-58L, 1958.
5. Driver, Cornelius: Longitudinal and Lateral Stability and Control Characteristics of Various Combinations of the Component Parts of Two Canard Airplane Configurations at Mach Numbers of 1.41 and 2.01. NASA MEMO 10-1-58L, 1958.
6. Spearman, M. Leroy, and Driver, Cornelius: Some Factors Affecting the Stability and Performance Characteristics of Canard Aircraft Configurations. NACA RM L58D16, 1958.
7. Foster, Gerald V.: Effects of Wing Vertical Location on the Stability and Control Characteristics at a Mach Number of 2.01 of a Canard Airplane Configuration With a Trapezoidal Aspect-Ratio-3 Wing. NASA TM X-44, 1959.
8. Spearman, M. Leroy: Investigation of the Aerodynamic Characteristics in Pitch and Sideslip of a 45° Sweptback-Wing Airplane Model With Various Vertical Locations of the Wing and Horizontal Tail - Effect of Wing Location and Geometric Dihedral for the Wing-Body Combination, $M = 2.01$. NACA RM L55B18, 1955.
9. Robinson, Ross B.: Effects of Vertical Location of the Wing and Horizontal Tail on the Static Lateral and Directional Stability of a Trapezoidal-Wing Airplane Model at Mach Numbers of 1.41 and 2.01. NACA RM L58C18, 1958.

03712201030

10

TABLE I.- GEOMETRIC CHARACTERISTICS OF MODELS

Body:

Maximum diameter, in.	3.33
Length, in.	37.0
Base area, sq in.	8.71
Fineness ratio	11.1

Wing:

Span, in.	16.72
Root chord at body center line, in.	22.97
Tip chord, in.	0
Area, sq in.	192
Aspect ratio	1.46
Taper ratio	0
Mean geometric chord, in.	15.33
Sweepback angle of leading edge, deg	70
Thickness, percent chord	2.5
Airfoil section	Hexagonal

Canard surface:

Total exposed area, sq in.	14.44
Ratio of exposed area to wing area	0.075
Section	Hexagonal
Maximum thickness, in.	0.3125
Sweepback angle of leading edge, deg	70

Vertical tail:

Panel exposed area, sq in.	23.42
Sweepback angle of leading edge, deg	60
Panel aspect ratio	1.11
Taper ratio	0.314
Airfoil section	Wedge-slab
Leading-edge wedge angle, deg	10.6
Constant thickness, in.	0.1875

L
4
9
4

DECLASSIFIED

11

TABLE II.- BODY COORDINATES

Body station	Radius
0	0
.297	.076
.627	.156
.956	.233
1.285	.307
1.615	.378
1.945	.445
2.275	.509
2.605	.573
2.936	.627
3.267	.682
3.598	.732
3.929	.780
4.260	.824
4.592	.865
4.923	.903
5.255	.940
5.587	.968
5.920	.996
6.252	1.020
6.583	1.042
17.75	1.667
37.00	1.667

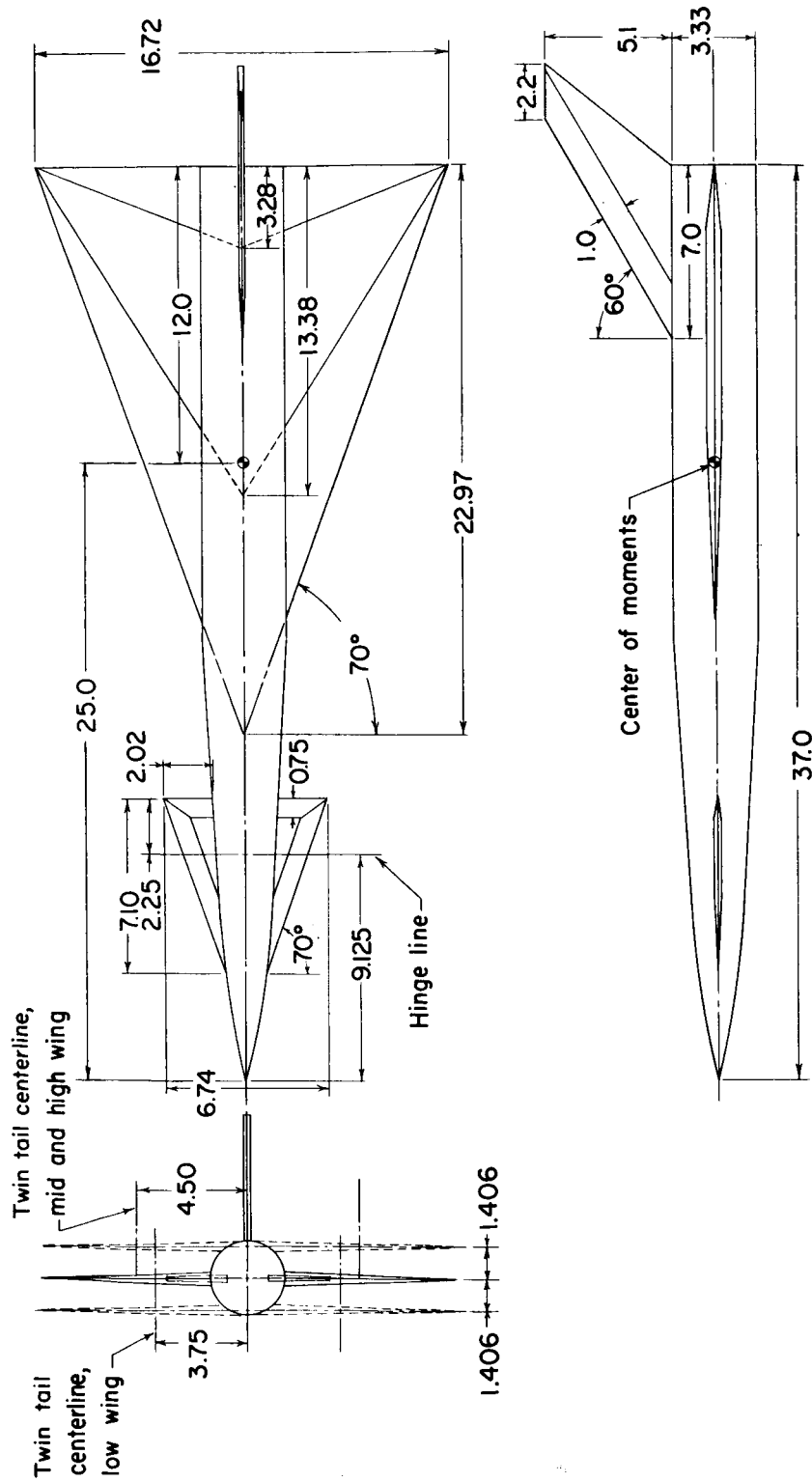
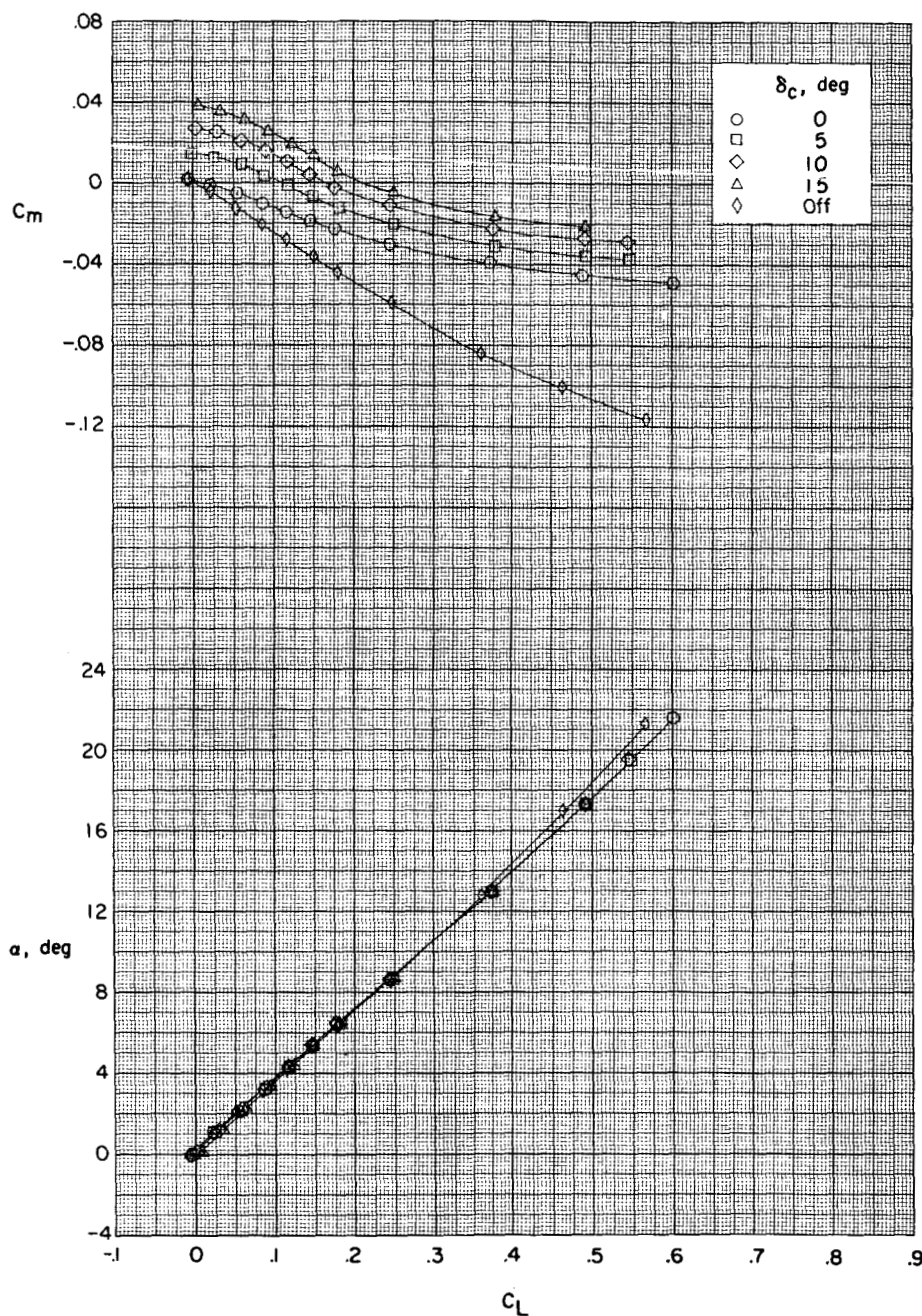


Figure 1.- Details of model. Linear dimensions in inches.

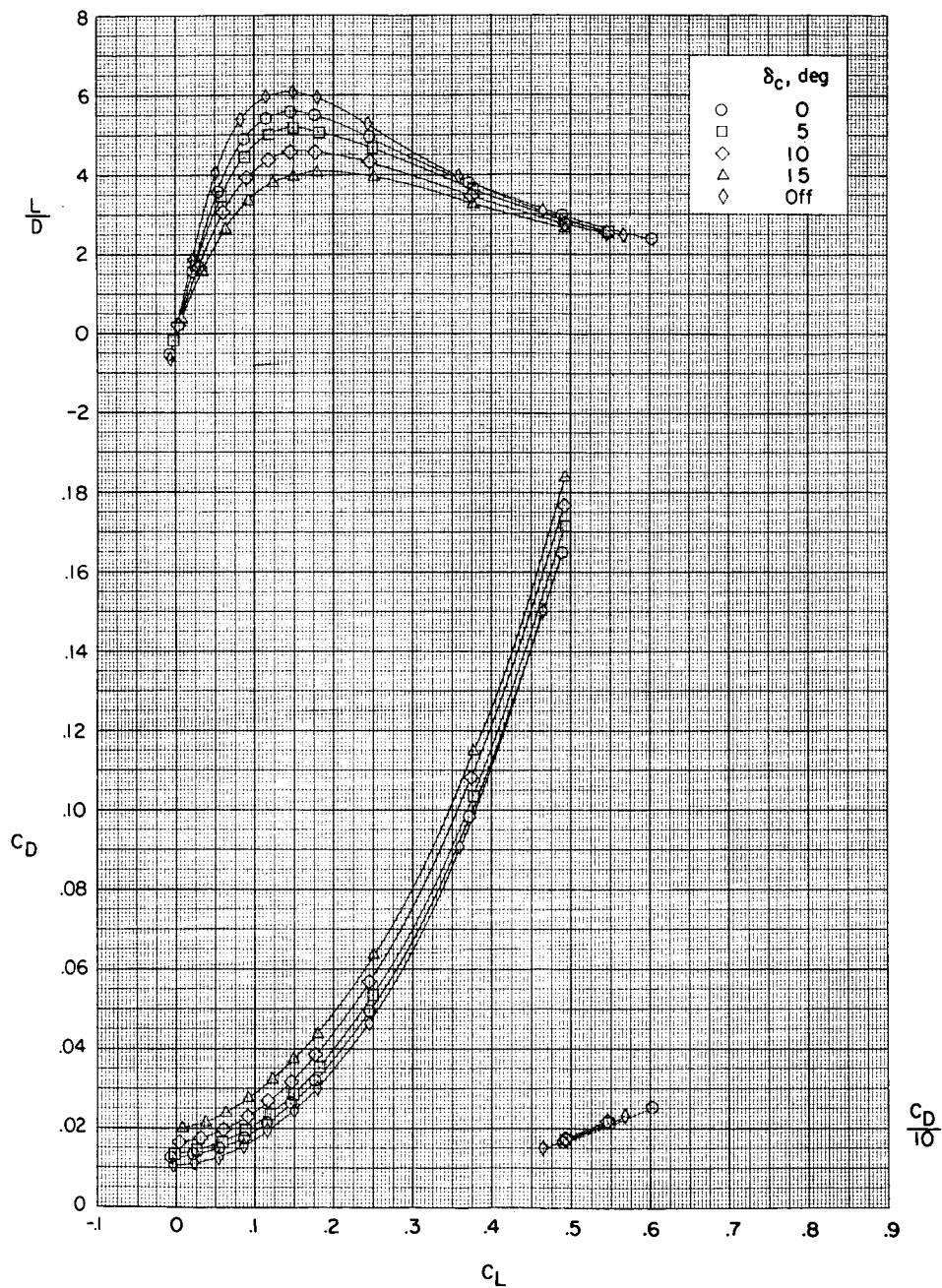


(a) High wing location.

Figure 2.- Effects of canard deflection on aerodynamic characteristics in pitch for various vertical locations of the wing. Single vertical tail on body.

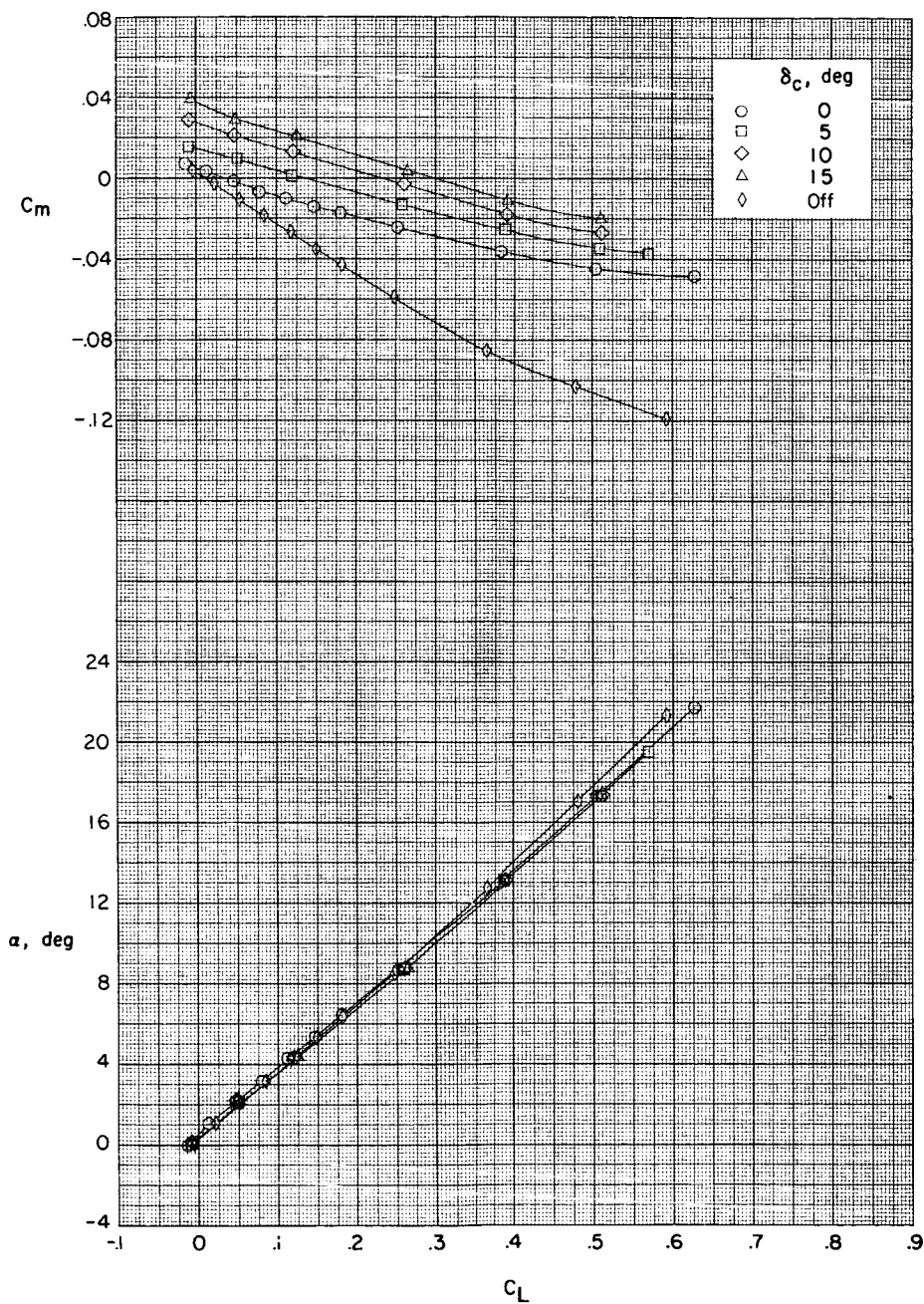
03:41:29.1030

14



(a) Concluded.

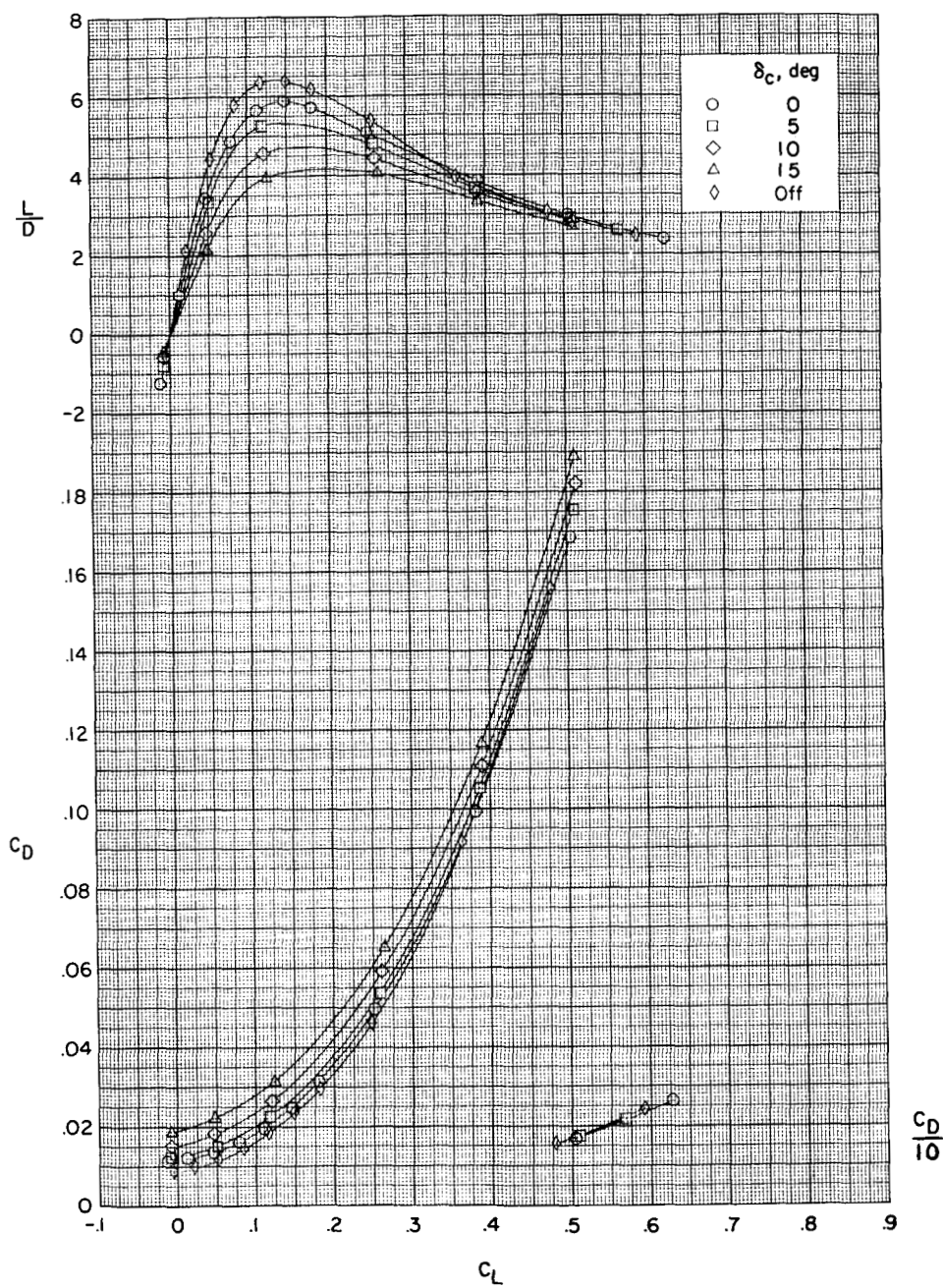
Figure 2.- Continued.



(b) Mid wing location.

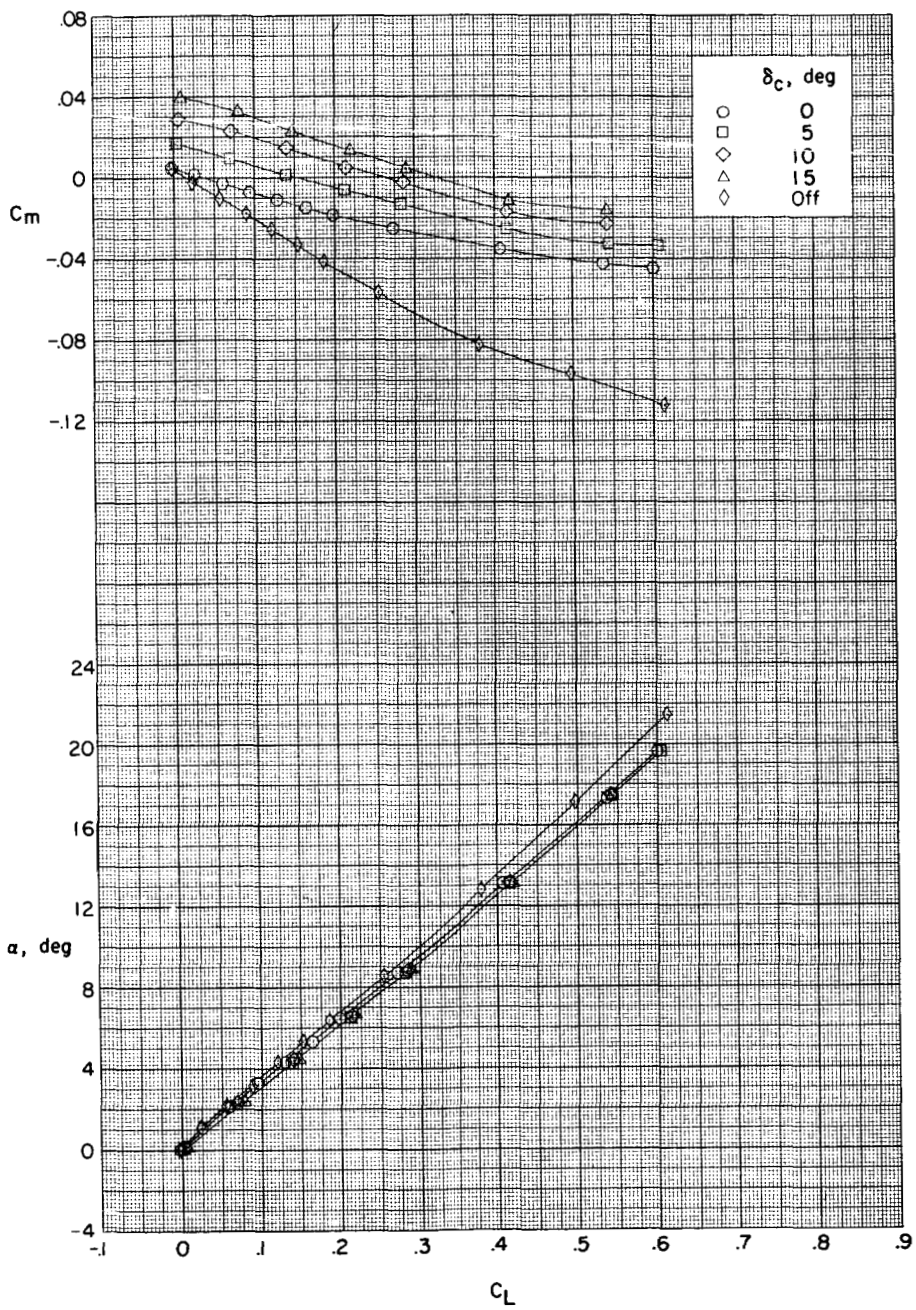
Figure 2.- Continued.

0371200.000



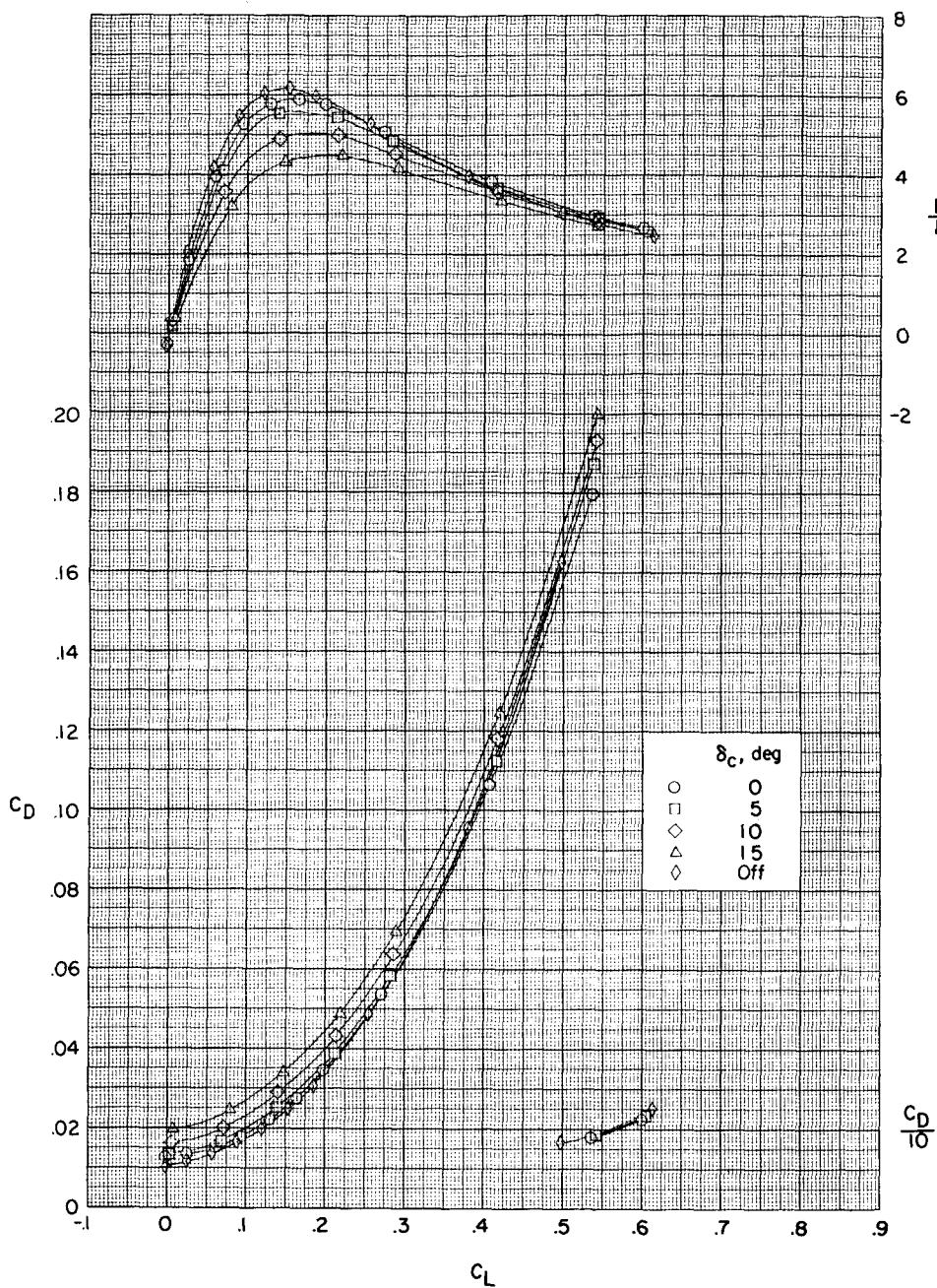
(b) Concluded.

Figure 2.- Continued.



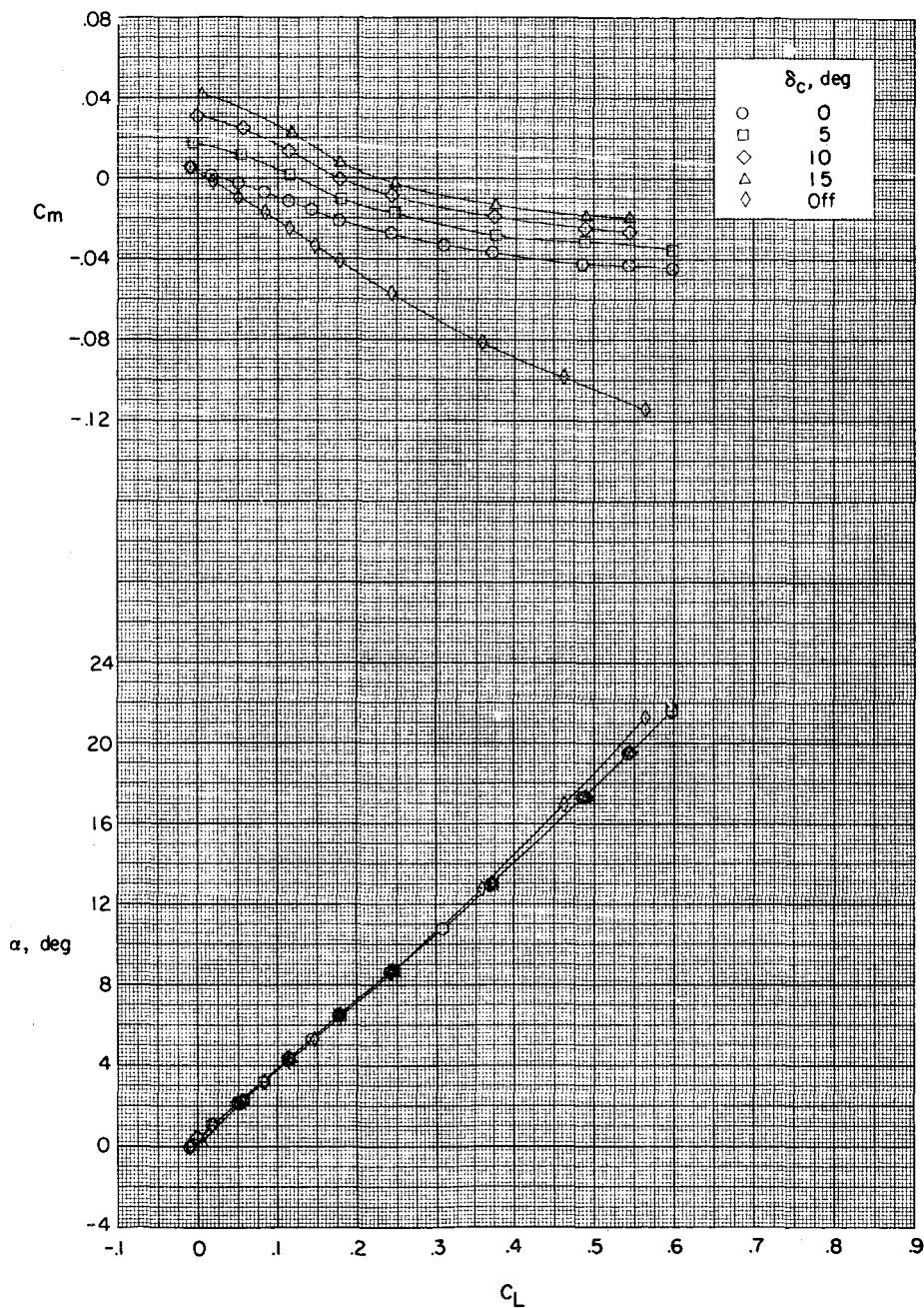
(c) Low wing location.

Figure 2.- Continued.



(c) Concluded.

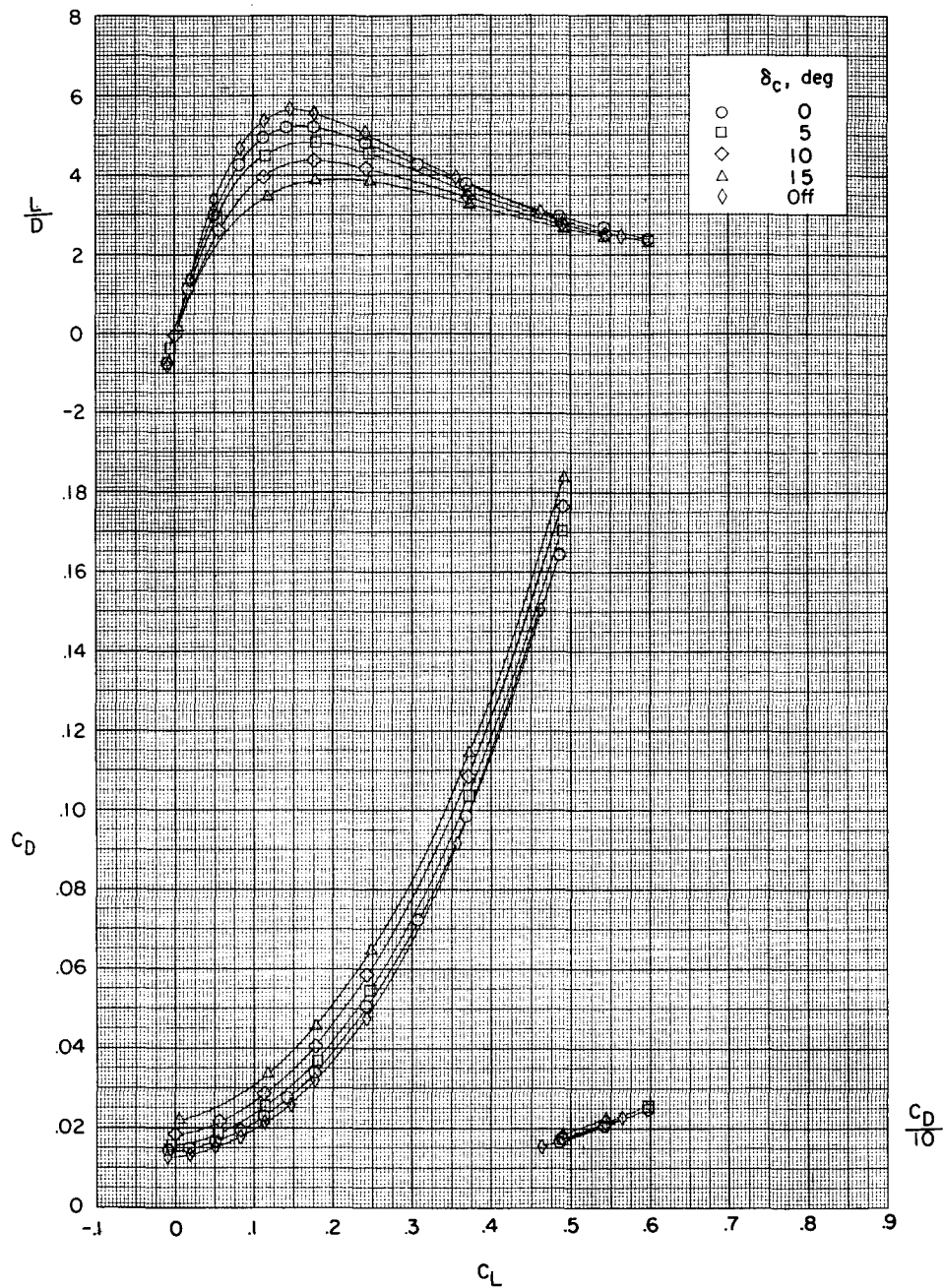
Figure 2.- Concluded.



(a) High wing location.

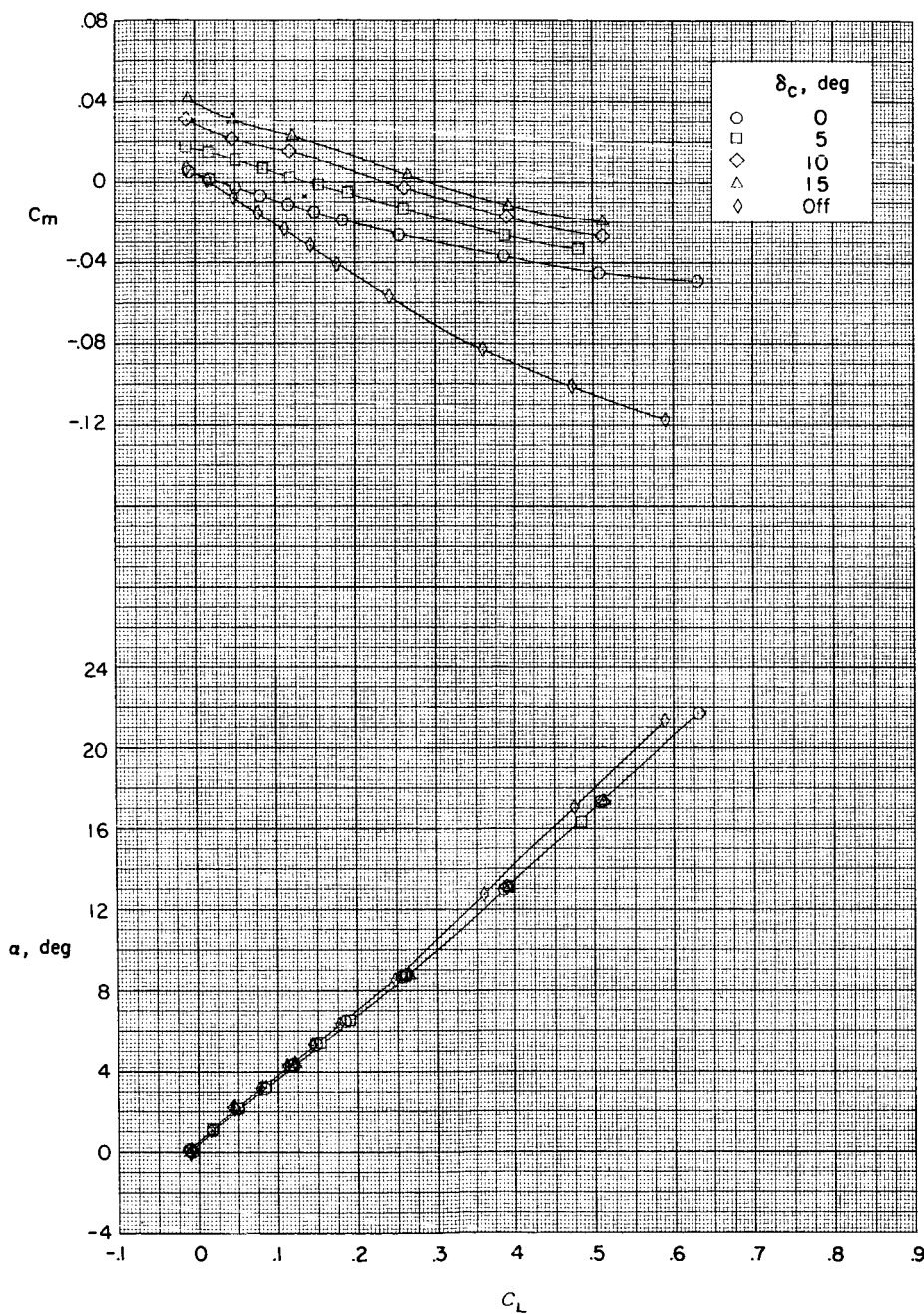
Figure 3.- Effects of canard deflection on aerodynamic characteristics in pitch for various vertical locations of the wing. Twin vertical tails on wing.

03720103



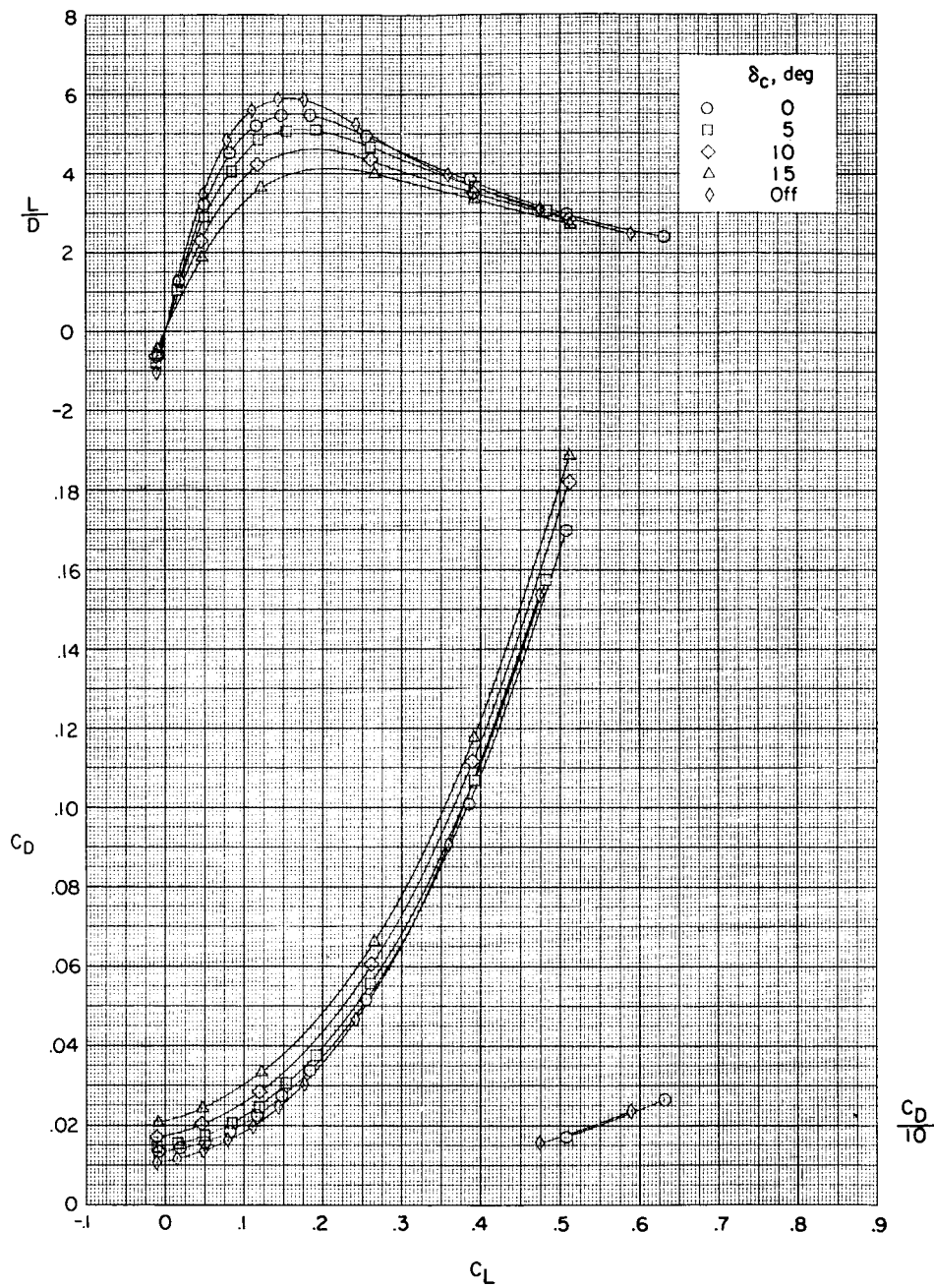
(a) Concluded.

Figure 3.- Continued.



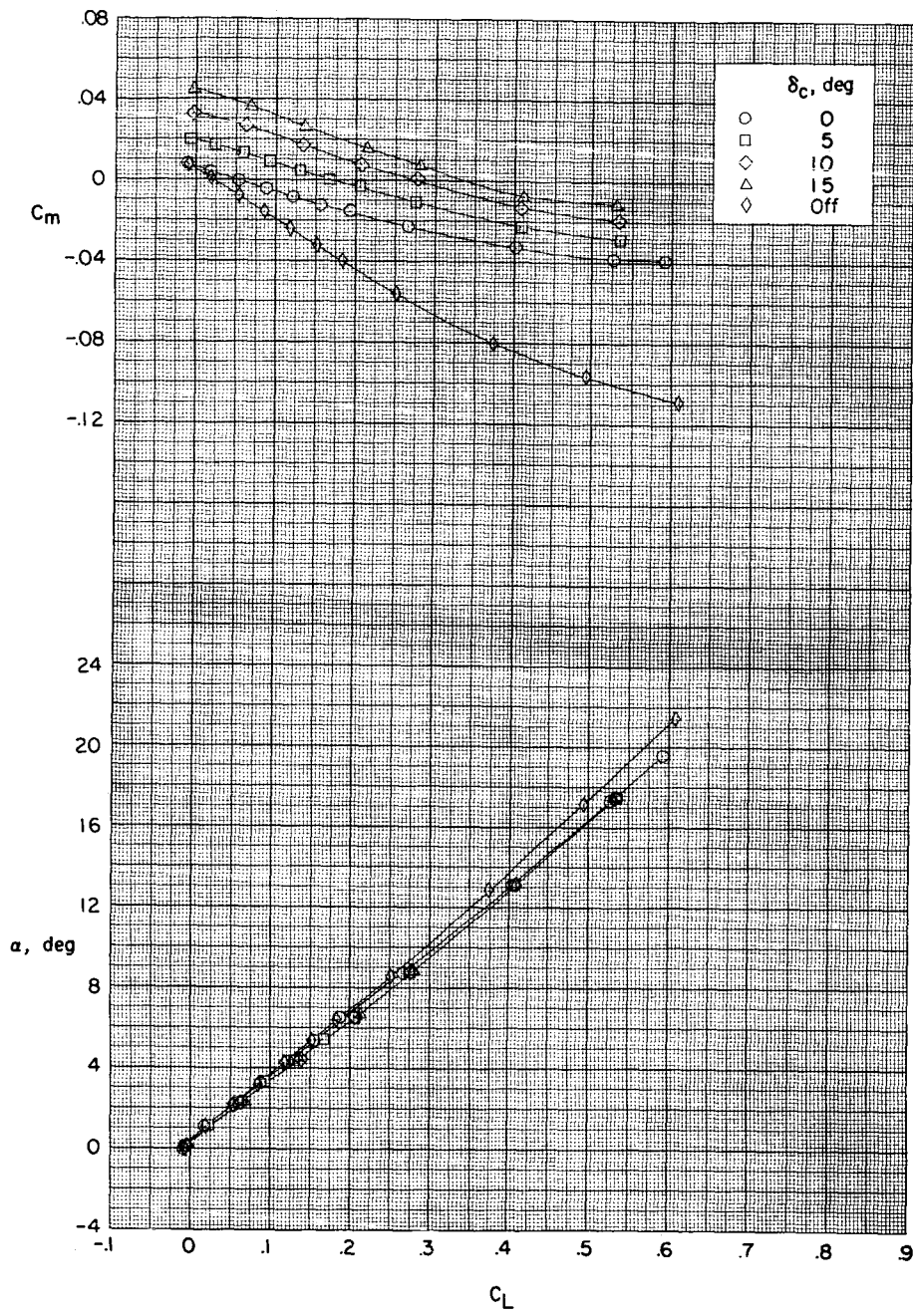
(b) Mid wing location.

Figure 3.- Continued.



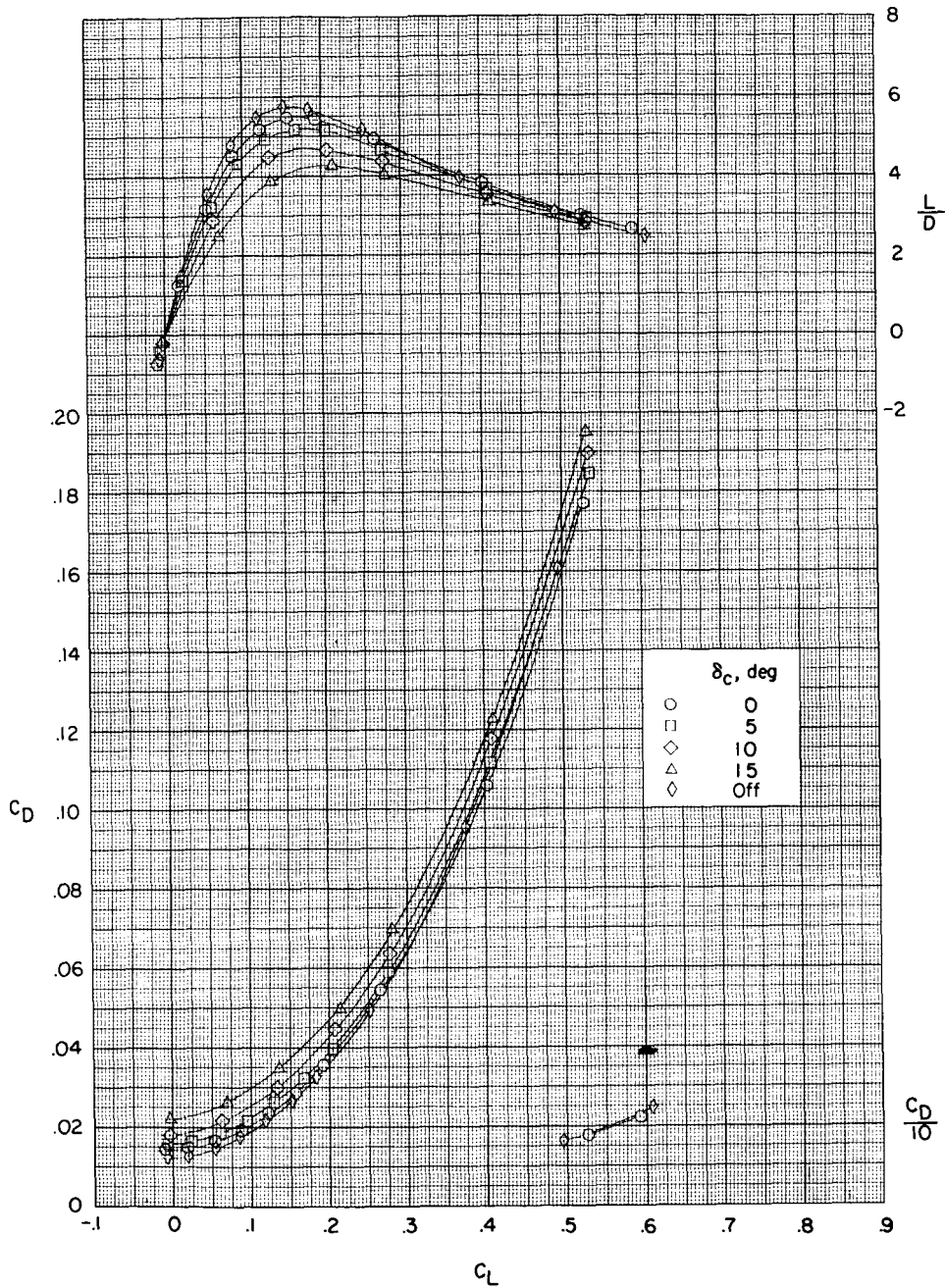
(b) Concluded.

Figure 3.- Continued.



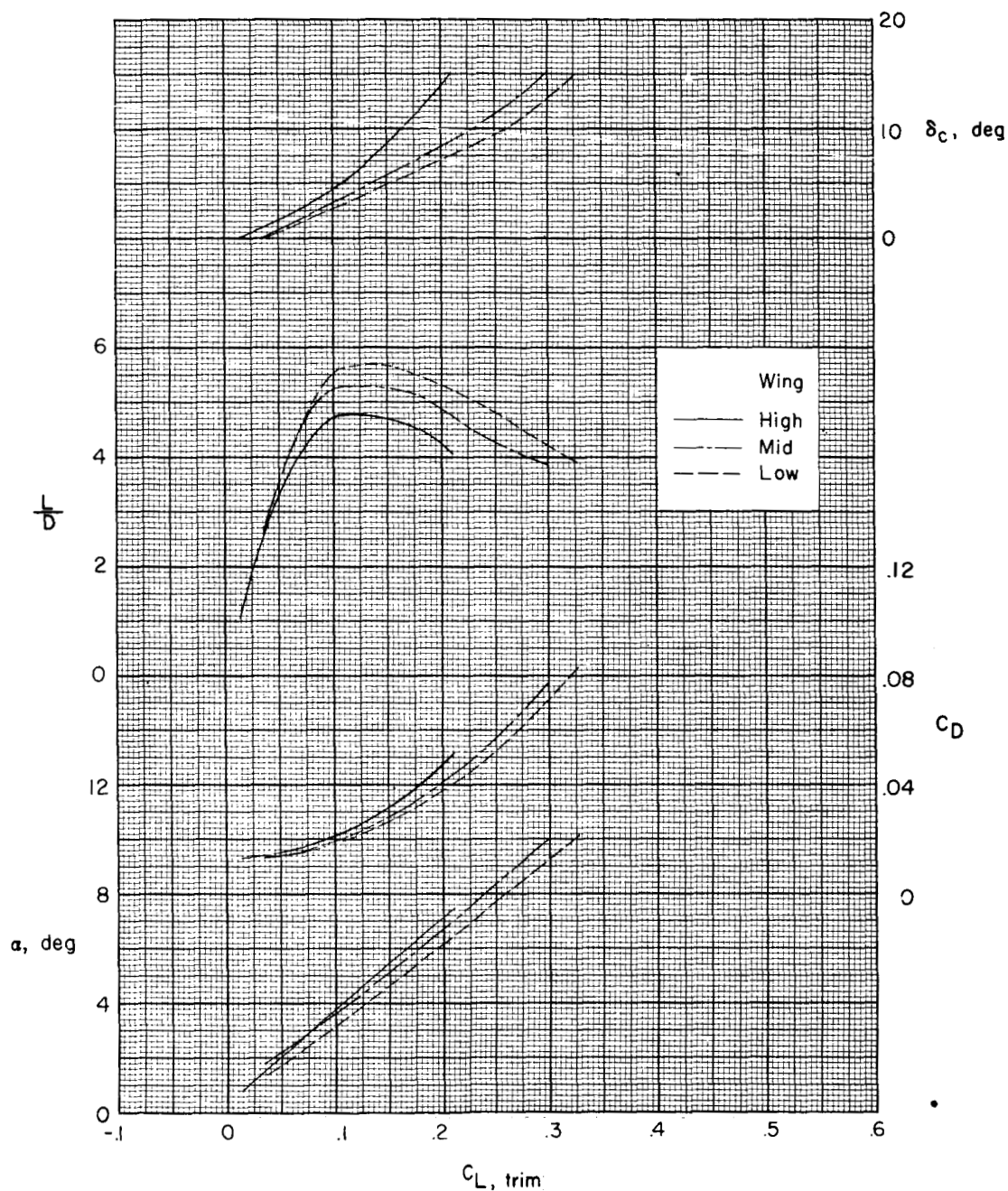
(c) Low wing location.

Figure 3.- Continued.



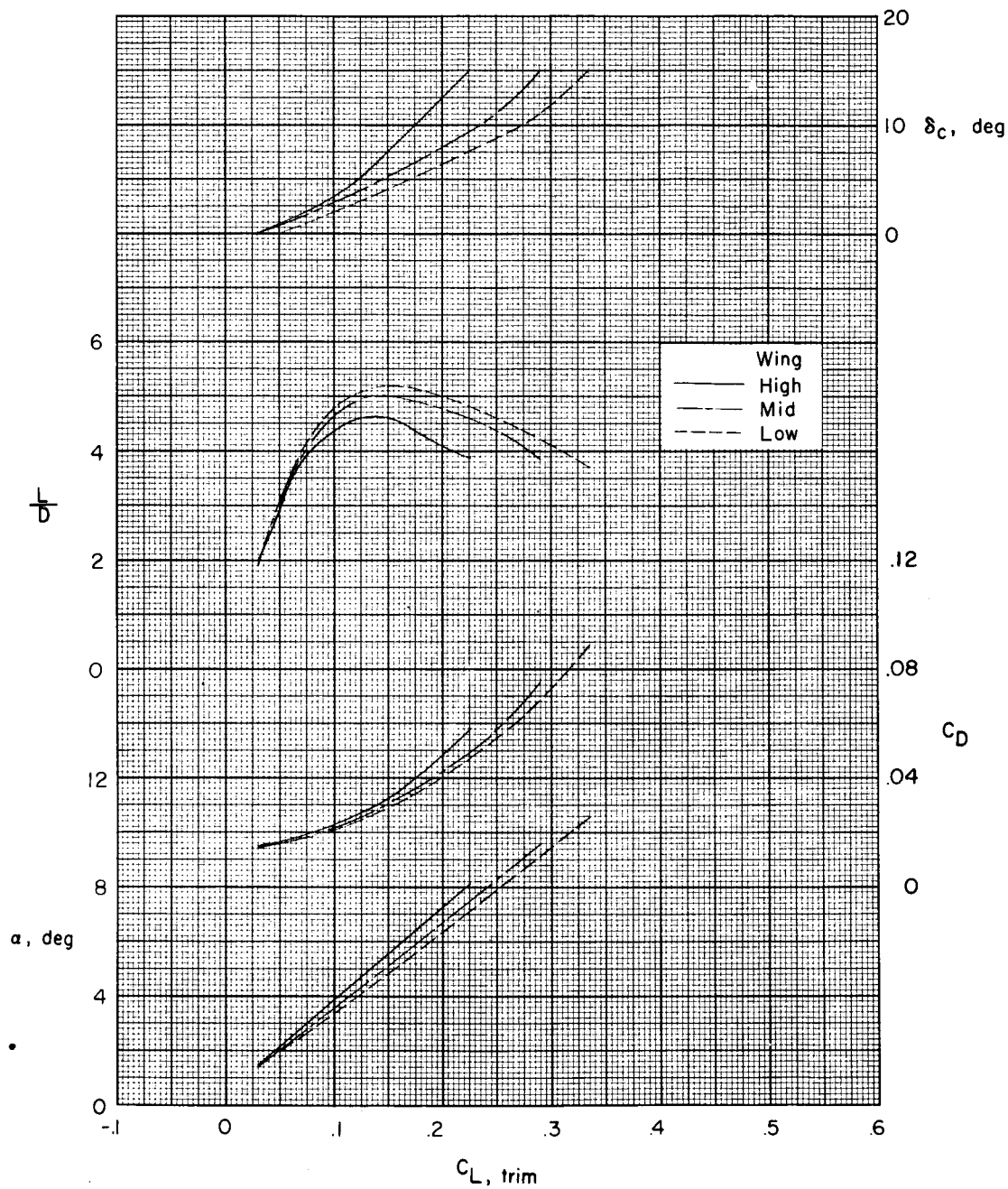
(c) Concluded.

Figure 3.- Concluded.



(a) Single vertical tail.

Figure 4.- Effect of vertical location of wing on trim longitudinal characteristics for a constant center-of-gravity position.



(b) Twin vertical tails.

Figure 4.- Concluded.

CONFIDENTIAL

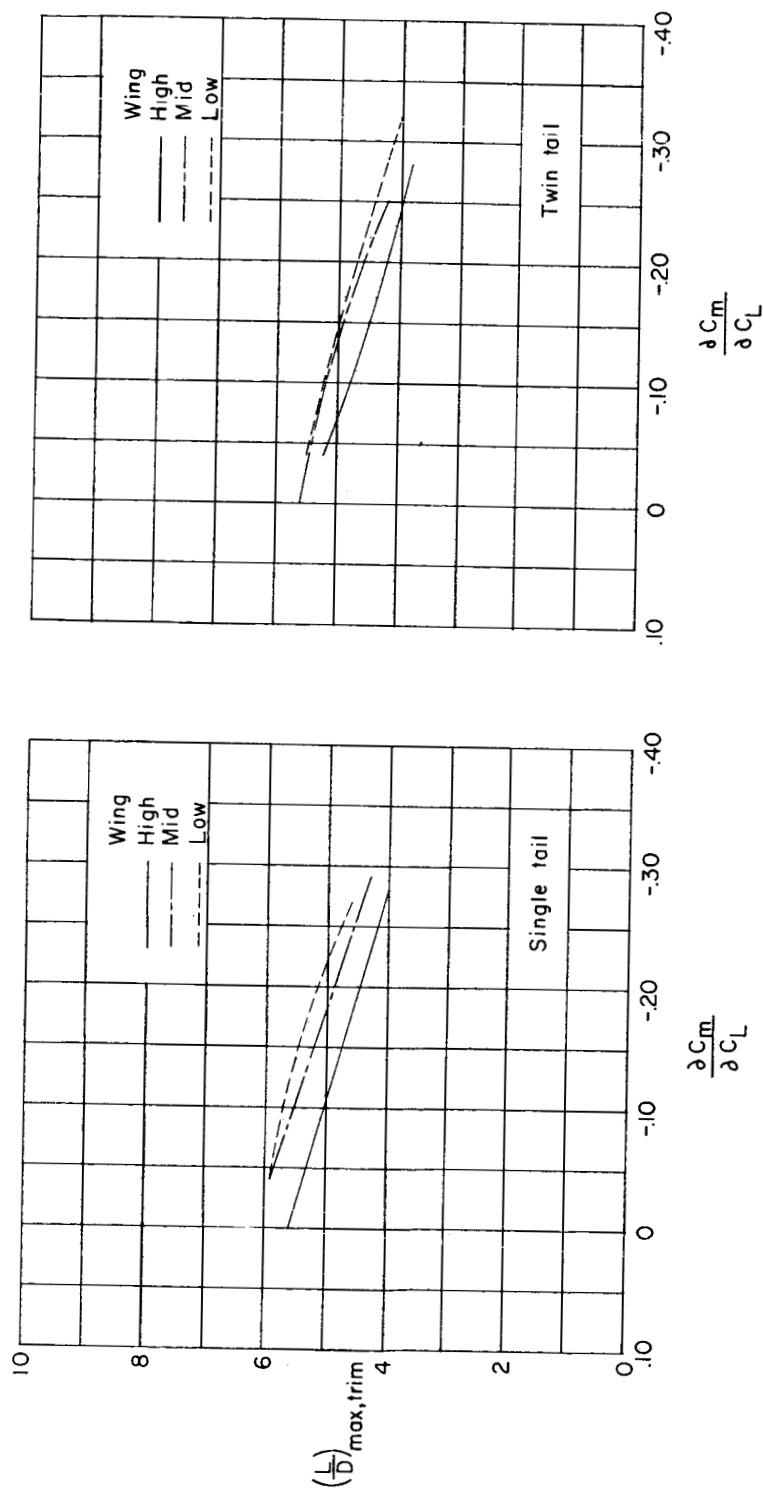
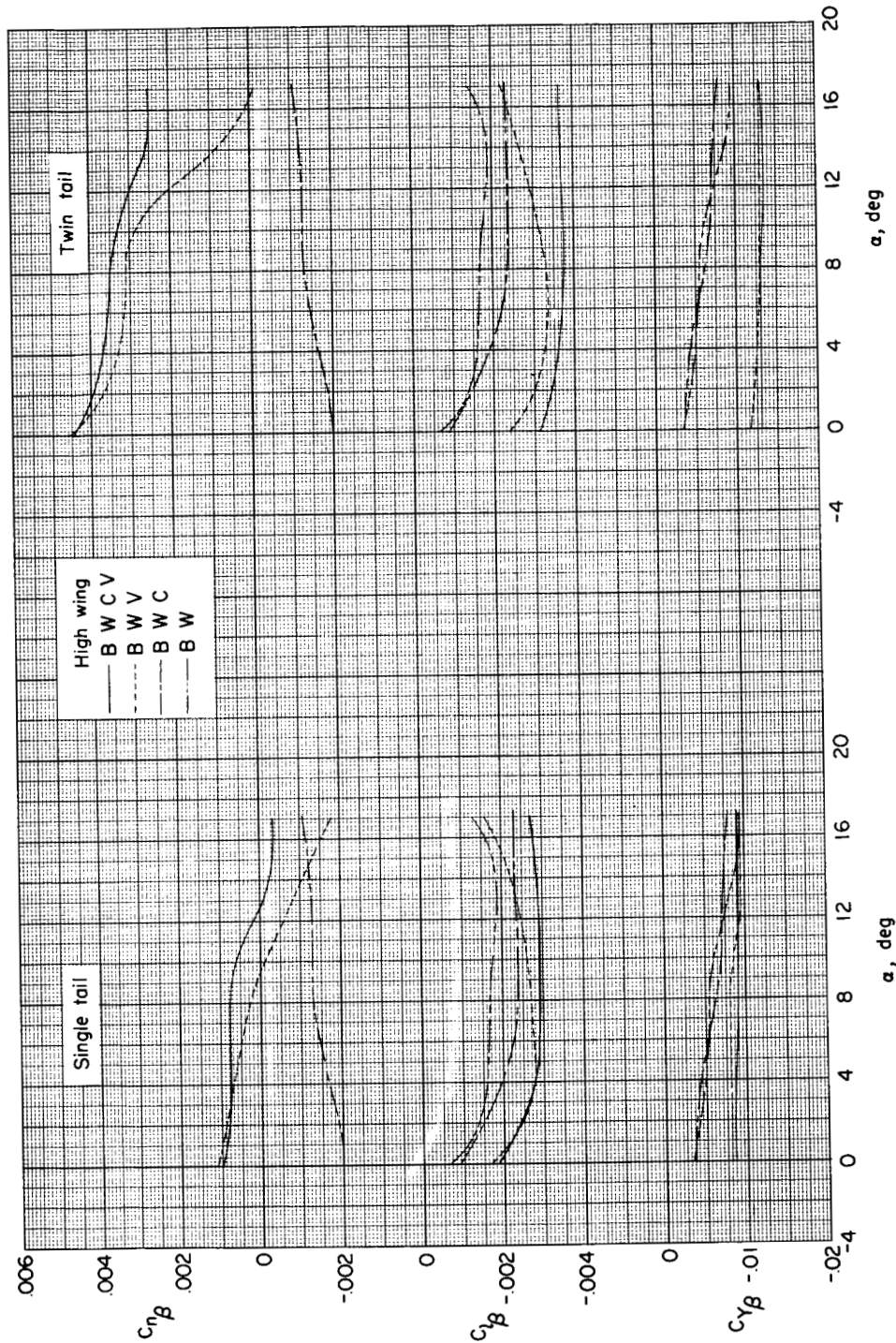
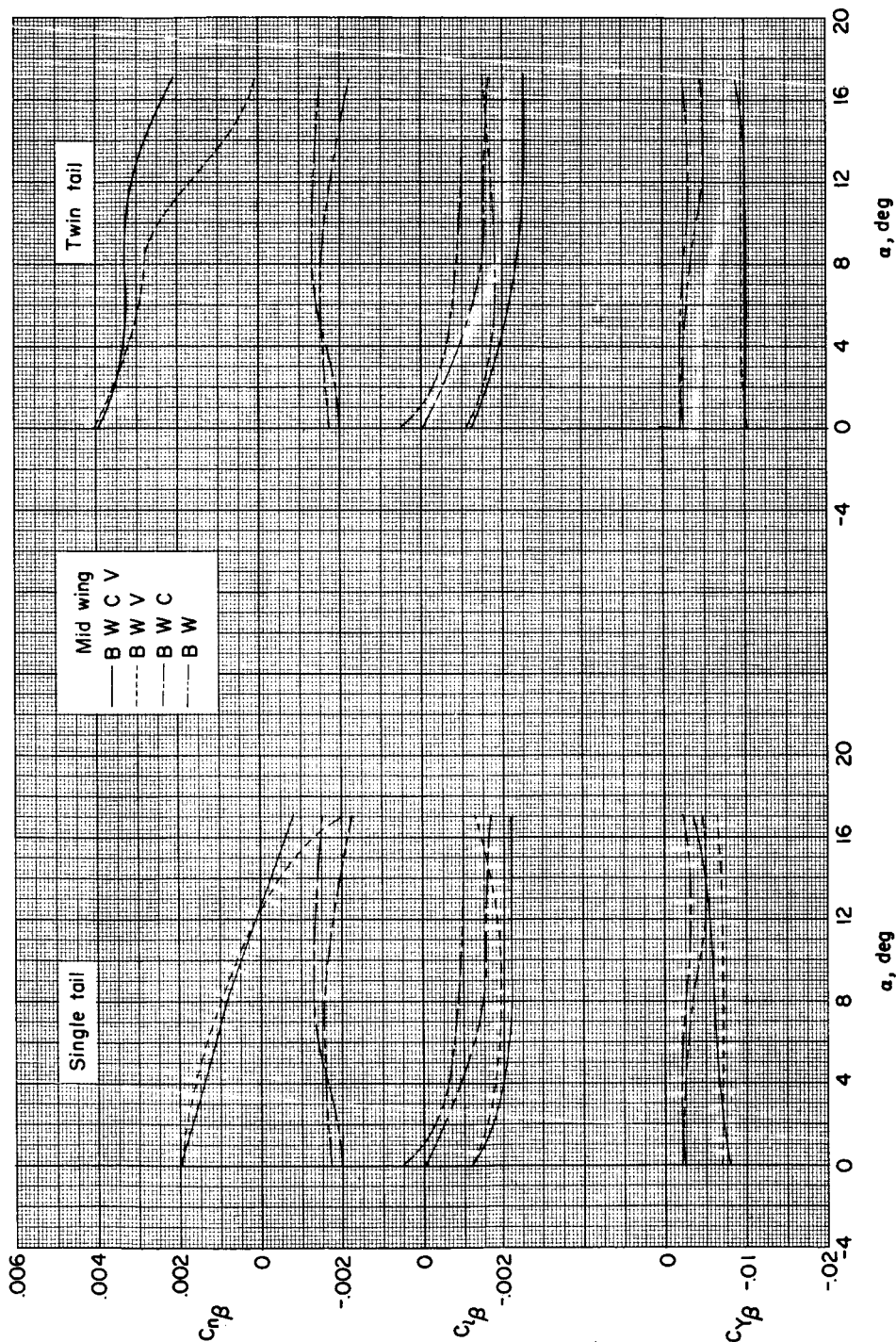


Figure 5.- Variation of maximum trim lift-drag ratio with longitudinal-stability parameter for various configurations.



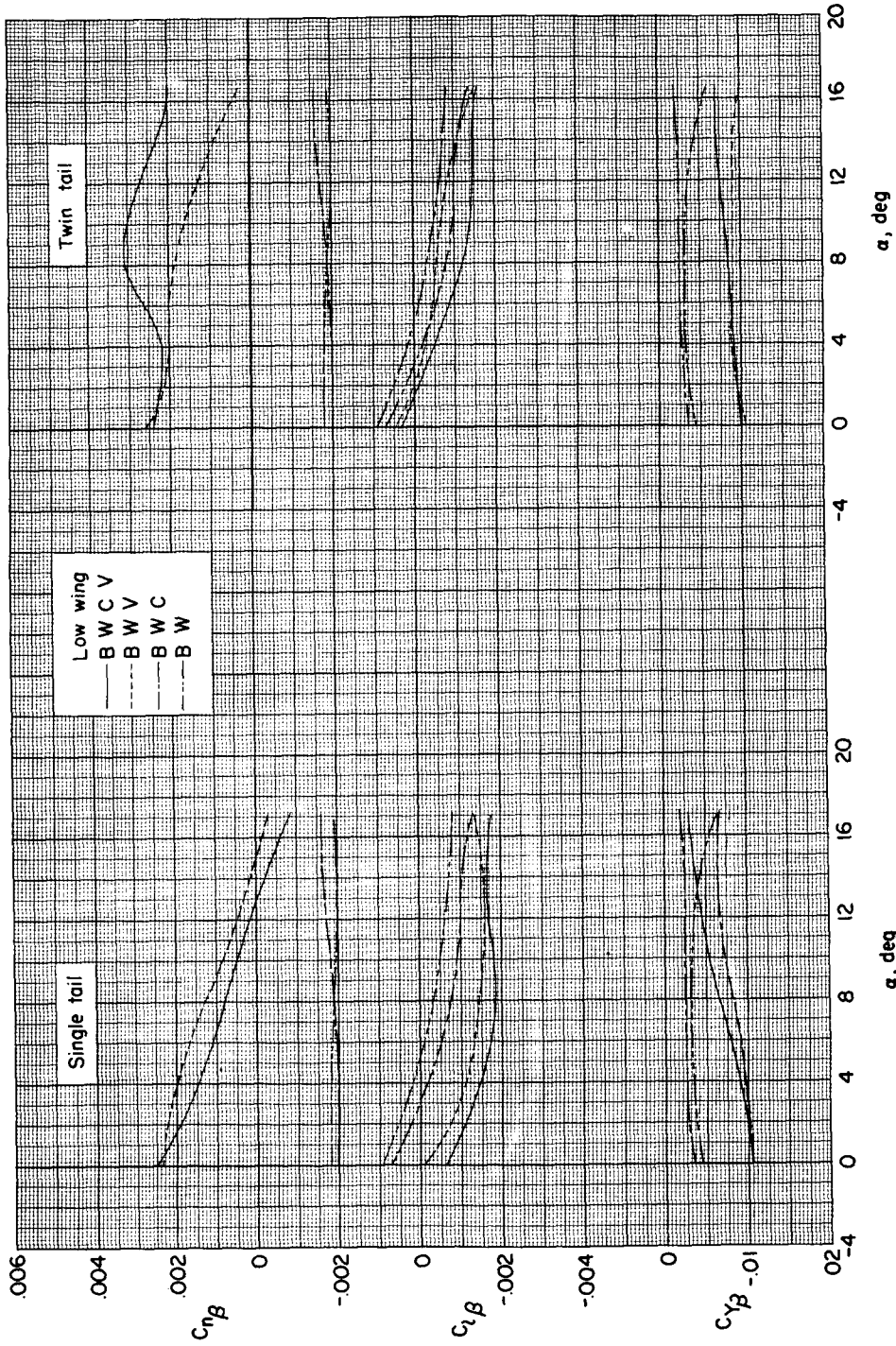
(a) High wing position.

Figure 6.- Effect of wing height on sideslip derivatives. (Tails on and off; canard surfaces on and off.) $\delta_c = 0^\circ$.



(b) Mid wing position.

Figure 6.- Continued.



(c) Low wing position.

Figure 6.- Concluded.